Year 24, Issue 1 June, 1979

The SPEX Speaker

SPEX INDUSTRIES, INC. - 3880 PARK AVENUE - METUCHEN, N. J. 08840 - ☎ (201) - 549-7144

A WINDOW INTO THE WORLD OF CELLS

R. Kaminski

At this very instant millions of cells in the lenses of your eyes are straining to focus the image of this page onto the photoreceptor cells of your retina. There the image is converted into impulses, then transmitted to your brain cells to be catalogued and stored as memory. Yet, even while these teaming ranks of microscopic vessels surge into the sensation of reading, untold billions of other cells go about their own special business of keeping you alive: dividing, growing, metabolizing, synthesizing, and yes, even dying.

Each of us, along with the towering oaks, the awesome dinosaurs and the ocean plankton, share a common experience. We all began life as a single cell that divided once, divided again, and relentlessly multiplied until descendants numbered thousands of billions. Locked into every one of these cells is a key to its proprietor's future, a genuine genetic copy complete with occasional misprints, flaws, and fortuitous accidents. Are we plant or animal, male or female, tall or short? Will we prematurely bald or will our eyesight falter? Will we fight off this cold, or catch something worse? Ask the cell. But be careful how you phrase that question!

We've been forewarned by the uncertainty principle: our probes may only find their own trails. Could we muster the ingenuity to enter a cell, our very presence would upset the works. So try the microscope. The light microscope that brought us cytology is limited in resolution to about 200 nm and demands stained, thin specimens isolated from their natural environments. Electron microscopes are more powerful, delivering about 1 nm resolution—a typical dimension of biological macromolecules—but they insist on even thinner specimens. And bombarding a sample with high-energy electrons is not always a good idea when you're trying to expose the fragile maze of interactions that make the cell work. What we really need is a one-way window into this corpuscular world, to watch the cell as it works and goes about its tasks oblivious of us and the tools of our curiosity.

In a manner of speaking spectrofluorescence [1,2] offers a collection of such windows into the cell. Presenting the different vistas is the SPEX FLUOROLOG's array of sources,

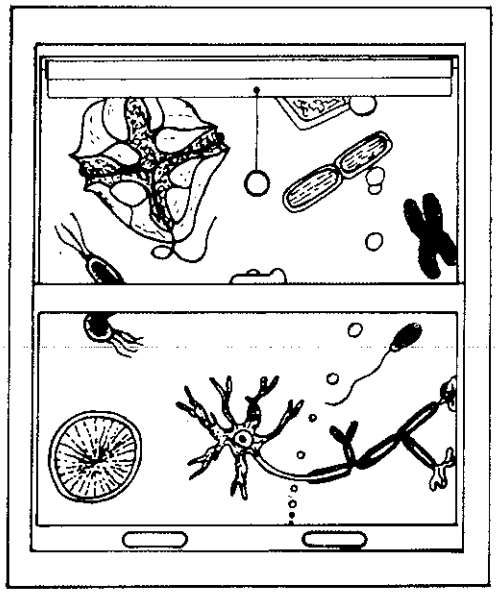

operating modes, detectors, and accessories. With both emission and excitation fluorescence spectra sensitive to minute variations in the environment of a molecule, chemical events in living cells can accurately be monitored. In particular, changes in intensity, peak position, lifetimes, and polarization will each reveal separate cell functions. And although all things do not fluoresce, attaching fluorescent probes (chromophors) to molecules without altering their chemical properties is now a standard and powerful laboratory technique. Exploited with the conveniences of the FLUOROLOG, chromophore methodology has invaded the privacy of cell walls.

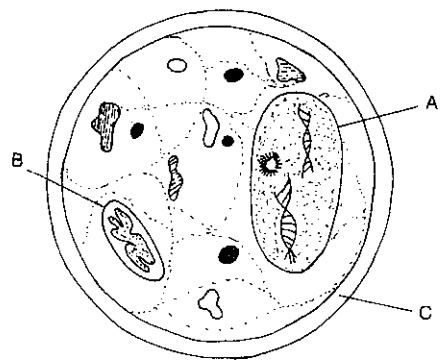

Fig 1 A typical cell is composed of three basic structures: (A) the nucleus that manufactures RNA and is the custodian of the genetic code; (B) the cytoplasm including the lysosomes and mitochrondria where digestive and energy-transforming reactions take place; and (C) the cell membrane that controls the environment in the cell interior through selective permeability. Thin membranes tend to be spherical since this shape is most economical (the law of minimal surfaces) [3].

The Cell Doctrine

As far as anyone can tell, Robert Hooke (of Hooke's Law fame) became the first person to peer into cell superstructure when he focused his crude microscope on thin slices of cork in 1665. He noted that the cork, rather than being a continuous, homogeneous material, was actually segregated into tiny pockets he dubbed cells, or pores. Expanding this investigation, he discovered that this architecture was not unique to cork. The same "Schematisme" appeared in the pulp or pith of other plants and vegetables.

The concept of the cell as the fundamental unit of life, however, did not surface until 1839 when M.J. Schleiden and Theodor Schwann advanced what was soon to become the kernel of modern biological theory. Within twenty years, Rudolf Virchow began the original which-came-first controversy when he concluded that cells arise only from other cells. From that time on, life was recognized as an unbroken cycle of cell division and growth.

Cell sizes range from a 100 nm pneumonia bacterium to a 15 cm ostrich egg; and each type of cell is different. Nerve cells, for instance, can stretch to one meter in length but become so thin they can't be detected with the naked eye. Still some features are common to all cells (Fig 1).

The nucleus is the central control for reproduction, carrying the genetic template DNA (deoxyribose nucleic acid) which synthesizes the RNA (ribonucleic acid) which in turn herds amino acids into the proteins that are essential for life. The nucleus floats in a mass of cytoplasm that is further divided into subunits of large, complex molecules such as lysosomes (the pockets of digestive enzymes that render large fat molecules) and the mitochrondrion (the cell's powerhouse where fuel molecules are oxidized and the energy distributed).

Enveloping this minute efficient, biological factory is the cell wall or membrane, a multi-layered, semi-permeable bag that protects the interior and regulates which molecule can pass inside from the surrounding medium and which are excluded. On the cell wall rests the responsibility to maintain a hospitable, controlled environment inside the cell.

Mad Dogs and Micelles

Call something hydrophobic and most people conjure up a vision of canine incisors dripping with white foam. But to a biochemist, the hydrophobic effect is the primary factor governing the structure and formation of cell membranes. Though life (on earth at least) cannot survive without water, some processes thrive without it, as we shall see.

A hydrophobic molecule is one that is insoluble in polar solvents (those composed of molecules with asymmetric charge distributions) such as water, though it may mix well with other non-polar solvents like ether. On the other hand, a hydrophilic molecule is ionic or strongly polar and thus tends to merge eagerly with water. When molecules have a dual nature, one end hydrophilic (head), the other hydrophobic (tail), they are ambivalent in aqueous solutions, one end attracted to the water, the other repelled. If the tails of these amphiphiles are hydrocarbon chains, they will also tend to aggregate, forming vesicles such as in Fig 2A, with the heads on the exterior. Due to the affinity of the tails for one another, the center of these structures, known as micelles, remains in a fluid, deformable state. Bile salts, for instance, form micelles to help break down fats and fat-soluble vitamins.

Amphiphiles with two hydrocarbon tails per head behave somewhat differently, collecting in large, planar bilayers which can fold into essentially spherical vesicles with solvent-filled interior cavities and head groups lining the inner and outer surfaces. This behavior is analogous to that of certain lipids (biological molecules soluble in organics but not water), including fats and hormones, when they unite to form the cell membrane. Thus, with the proper choice of amphiphilic molecules, we can produce membranes that mimic cellular construction and, with these models, isolate cell processes for individual analysis.

Phosphorescence and Fluorescence

With the membrane in control of the cell's environment, molecules and salts essential to metabolism are granted free passage while undesirables are normally rejected. Unfortunately, some carcinogens, such as benzopyrene, are able to penetrate cell defenses. Recently, Turro and Aikawa, at Columbia University [4], have begun to clarify some of the questions surrounding this sequestering ability of cell membranes. With micelles as models, they examined the emission spectra and lifetimes of molecules that were selectively organized into the protective membrane interiors. Then, by varying the concentration of quenchers in the exterior medium while observing alterations in the fluorescence, they were able to estimate the rate of diffusion of the molecules across the cell boundary.

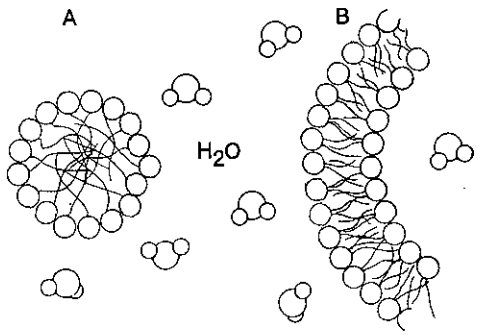

Fig 2 Molecules with a hydrophobic tail and a hydrophilic head tend to aggregate into micelles (A). Molecules with two tails (B), may form bilayer sheets that can fold into spheres with water filling the cavity inside.

In an elegant, deceptively simple experiment, they produced micelles from sodium dodecyl sulfate (SDS) and introducted 1-chloronapthalene into the solution. 1-chloronaphthalene both fluoresces (10^{-8} sec lifetime) and phosphoresces (milliseconds) though the latter is weak in aqueous solutions due to quenching by species that tend to deactivate the triplet state responsible for phosphorescence. Micelles, however, protect the molecules by sequestering them and the phosphorescence is readily observed in these solutions, even at room temperature. When solutions are examined with the 1934 Pulsed-lamp Phosphorimeter accessory to the FLUOROLOG [5], a few microseconds delay inserted between excitation and sampling should theoretically allow the fluorescence to decay and leave only the more persistent phosphorescence spectra. Yet, when the spectra were actually run, peaks identical to the fluorescence bands appeared (Fig 3), despite delays as long as 1200 μsec!

What Turro and Aikawa were in fact seeing was a process called delayed fluorescence. Ordinary fluorescence is the result of transitions between excited singlet states and the ground state and therefore occurs quickly. In viscous media, such as the protected interior of a cell, however, some of the triplet-excited phosphorescence molecules live long enough to collide before they can emit. Upon impact, one molecule is knocked into an excited singlet state and from there fluoresces. The frequency of the resulting spectrum is therefore identical to that of normal fluorescence [6]. (The other molecule in the collision proceeds to the ground state through internal conversion.) This triplet-triplet annihilation process is just the one experienced by 1-chloronaphthalene in the spectra of Fig 3. Notice how the variation of sampling and delay times discriminates against one type of luminescence at the expense of the other, according to their lifetimes. Waiting only briefly before taking a quick look at the detector signal favors the shorter-lived delayed fluorescence. Extending both delay and sampling times tips the balance in favor of the phosphorescence.

Though delayed fluorescence is recognized to be the source of the luminescence, the specific route to triplet-triplet annihilation can take any of the three forms shown in Fig 4. In (A), two separate micelles containing excited 1-chloronaphthalene molecules

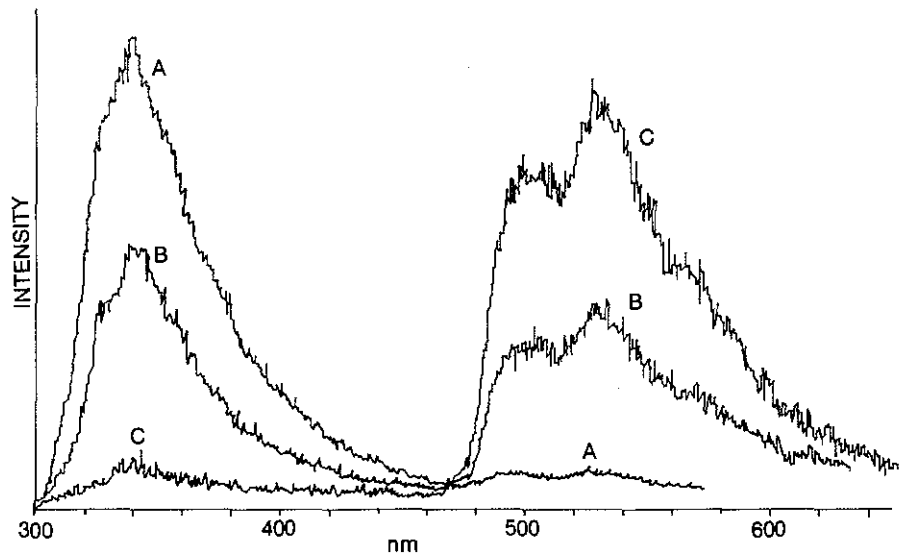

Fig 3 Time-resolved spectra of 1-chloronaphthalene in sodium dodecyl sulfate. The emission from 300-450 nm is delayed fluorescence, thet above 450 nm is phosphorescence. In (A), the delay between excitation at 305 nm and the 200 μsec sampling period was 30 μsec. In (B), sampling time was 1000 μsec, delay 200 μsec. In (C), delay has been extended to 1200 μsec and sampling to 1500 μsec. The lifetime of the phosphorescence is about twice that of the delayed fluorescence.

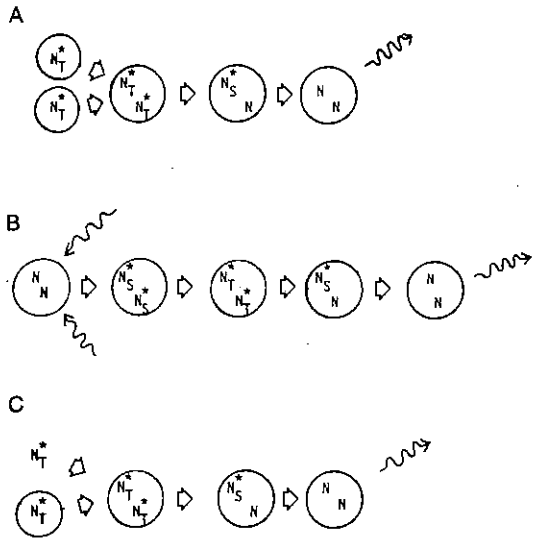

Fig 4 Three proposed mechanisms leading to the triplet-triplet annihilation responsible for delayed fluorescence. In (A), two excited molecules in separate micelles collide, the micelles merge, annihilation occurs. In (B), two molecules occupying the same micelle are excited. In (C), an excited molecule from the surrounding medium penetrates a micelle containing another excited molecule.

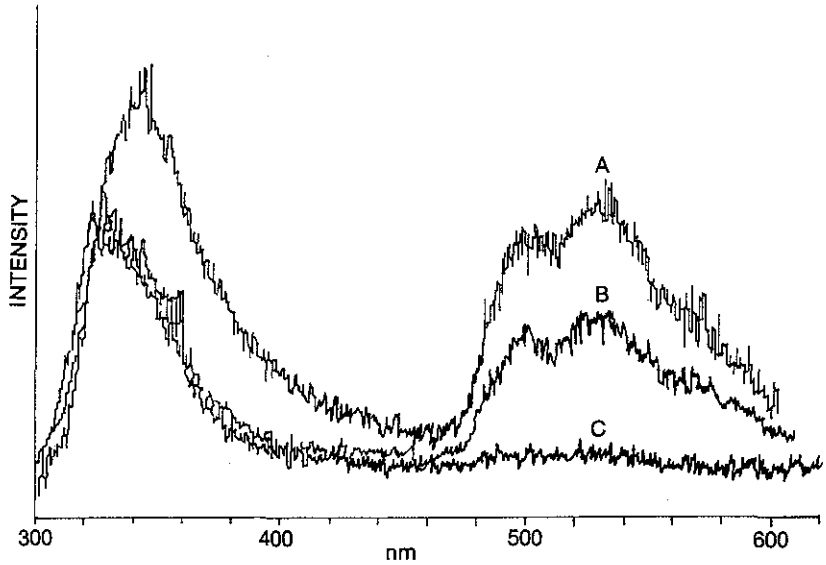

Fig 5 Spectra of micellar 1-chloronaphthalene as a function of the concentration of $NaNO_2$, a quencher of phosphorescence triplet ststes: (A), no quencher, (B), 10^{-4}M $NaNO_2$; (C), 10^{-3}M $NaNO_2$. As more quencher is sdded the ratio P/F decreases contrary to expectations if (C) in Fig 4 were the primary mechanism for triplet-triplet annihilation.

collide and merge before annihilated molecules can produce the delayed fluorescence. In (B), the molecules already occupy the same micelle before excitation occurs. Finally, an excited molecule in the surrounding medium penetrates a micelle containing another excited molecule (C).

If (C) were the primary source of the delayed fluorescence, the addition of a quencher to the solution would greatly diminish the number of excited molecules in the surrounding medium that survive long enough to penetrate the micelle. The molecules within the micelle would be protected from quenching, as indicated before, so they would survive long enough to phosphoresce and the intensity ratio of phosphorescence to fluorescence (P/F) should increase with the amount of quencher. Fig 5, however, demonstrates just the opposite: phosphorescence is eventually smothered by the quenching species, $NaNO_2$.

If (A) were the culprit, then, as the micellized solution is diluted, the chance for collisions between micelles containing excited molecules should decrease and, as before, P/F would be expected to increase. However, Fig 6 demonstrates that the contrary is again the case. Thus, the scheme depicted in Fig 4B must be the primary perpetrator in triplet-triplet annihilation of micellized 1-chloronaphthalene.

The extension of these results toward a general model of the cell could probably proceed from the Fig 5 data. The lifetime of a phosphorescing molecule is quite long, increasing the probability that it will leave the micelle and, no longer shielded, be quenched in the surrounding medium. On the other hand, once triplet-triplet annihilation occurs, the 1-chloronaphthalene molecules decay within a couple of nanoseconds. Thus, the lifetime of delayed fluorescence will be unaffected by quencher concentration, while the lifetime of phosphorescence will be modified accordingly. By varying the quencher concentration, the rate of crossing over the cell membrane can be determined. Extending these experiments to substances like benzopyrene will supply information on carcinogenic activity within the cell. Also, evidence exists [7] for the penetration of O_2 into the micelles and since oxygen is an effective quencher of the phosphorescence triplet state, quantitative data on the processes of oxidation and metabolism may be obtained.

Energy Transfer

A further example of the micelle's proclivity for selectively and efficiently organizing its interior is presented by Escabi-Perez, Nome and Fendler [8], Texas A&M University, in their work on energy transfer from naphthalene to terbium ions. Normally, terbium ions absorb uv and visible radiation very weakly and, as a consequence, their emission spectrum is feeble . . . even when the terbium is protected by SDS micelles. Naphthalene, on the other hand, exhibits strong absorption bands throughout this region and its excited triplet states are buffered in the presence of micelles. Introducing both terbium and naphthalene into an SDS solution alters the luminescence of each. The terbium phosphorescence intensity increases as a function of naphthalene concentration and new lines appear in the terbium excitation spectrum that correspond exactly to those of naphthalene. What happens here is that the emission bands of triplet naphthalene overlap the excitation bands of terbium, and since both are triplets and of the same symmetry, they interact readily, the naphthalene serving as a pump to populate the terbium excited states.

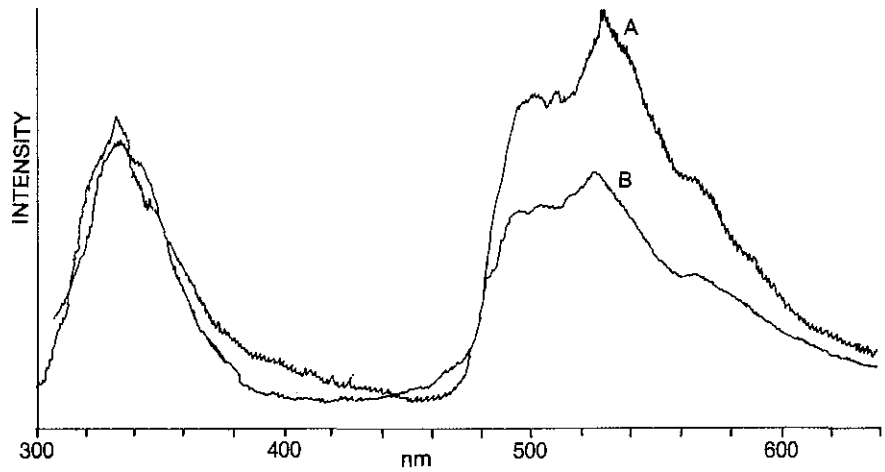

Fig 6 Spectra of micellar 1-chloronaphthalene as a function of concentration. (A) is a solution of 4.5×10^{-4} 1-chloronaphthalene in 0.050 M SDS. (B) is a solution 10 times ranfied. This dilution effect on the P/F ratio exonerates (A) in Fig 4 from responsibility for delayed fluorescence.

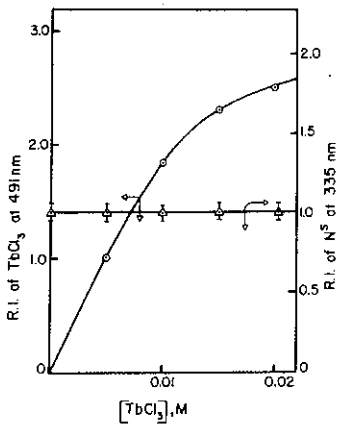

Fig 7 Plot of relative intensities of luminescence from $TbCl_3$ (triplet, o) and singlet naphthalene (Δ) in SDS as a function of $TbCl_3$ concentration. There is no evidence for energy transfer from the singlet to the triplet states.

Further evidence for the exclusive involvement of the triplet state in this energy-transfer process is given in Fig 7 where the relative intensity of the naphthalene singlet emission (fluorescence) is plotted along with the terbium emission (phosphorescence) as a function of terbium concentration. While the terbium emission shows undeniable increases, the naphthalene singlet is undiminished in intensity, indicating that it loses no energy to the enhancement process.

When terbium ions are introduced to micellized naphthalene, they migrate to the membrane surface (attracted by the micelle's negatively charged Stern Layer). Here they collect in close proximity to the naphthalene which can then supply them with the excitation energy they are incapable of absorbing for themselves. That this increased luminescence efficiency may some day lead to economical solar-energy conversion is appealing in itself [9, 10]. But more important to the cell story, the micelle's grouping together energy partners in this way qualifies it as an appropriate model for biological energy transfer.

Biological Energy Transfer

The primary pursuit of any cell is to transform energy so it can grow, eliminate waste, reproduce by splitting (mitosis), or simply move from one place to the next. Regardless of how this energy is obtained, it must be distributed. As we have seen, electronically excited molecules can yield their excess energy to other molecules through collisions or formation of complexes. However, molecules that are immobilized or separated by distances exceeding their diameters can also exchange energy efficiently [11] when the donor, in an excited state, acts as a charged oscillator, creating a field that extends out into the surrounding medium. When another molecule enters this alternating field, it begins to vibrate in sympathy with the excited molecule and if the frequencies between energy levels of the molecules are similar, the second molecule (acceptor) may be excited at the expense of the donor. Depending on the result, this process is called resonance transfer, or, when the acceptor is a fluorescent compound, sensitized fluorescence.

At Stanford University, Fung and Stryer [12] have developed a technique of fluorescence energy transfer with an eye toward determining the lateral distribution of lipids and proteins within cell membranes. Actual cell membranes are protein-lipid complexes that may contain up to 70% protein. Despite this, experimental evidence favors lipid bilayers as the predominant foundation of most membranes [13]. So charting the distribution of lipids and proteins in these structures is essential for modelling the cell.

For resonance energy transfer to take place, four conditions [14] must be satisfied:

1. The acceptor's absorption spectrum must overlap the donor's emission bands. Furthermore, the excited states of both molecules must be of like multiplicity, i.e., triplet (phosphorescence) or singlet (fluorescence).
2. The donor and acceptor oscillators must be favorably oriented to each other to allow strong interaction.
3. The excited state of the donor must be sufficiently long lived to make energy transfer practical.
4. For a given transfer efficiency, donor and acceptor must be within a certain distance.

Phosphatidylethanolamine (PE) and phosphatidylcholine (PC) are two lipids that are components of most animal membranes. That PE labelled with suitable chromophores satisfies the first condition when incorporated into bilayer PC vesicles can be seen in Fig 8. These fluorescence emission and excitation spectra of 2,6-dansylPE (2,6-DPE) and eosinPE (EPE) were taken on the Spex FLUOROLOG in the E/R (Emission/Reference) mode that automatically corrects for any variations in excitation radiation that might occur during a scan. Note that the full emission spectrum of 2,6-DPE overlaps the EPE excitation spectrum.

That the next two requirements are met can be appreciated from Fig 9 which displays emission spectra for a combined 2,6-DPE and EPE solution at various relative concentrations of PC to EPE. Note that energy transfer increased as the density of EPE in PC increased, even though the concentration of 2,6-DPE was kept constant.

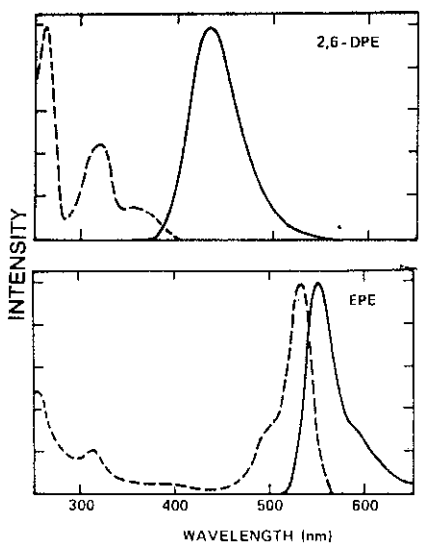

Fig 8 Excitation (---) and emission (—) spectra of 2,6-DPE and EPE in PC vesicles taken on the FLUOROLOG in the E/R mode.

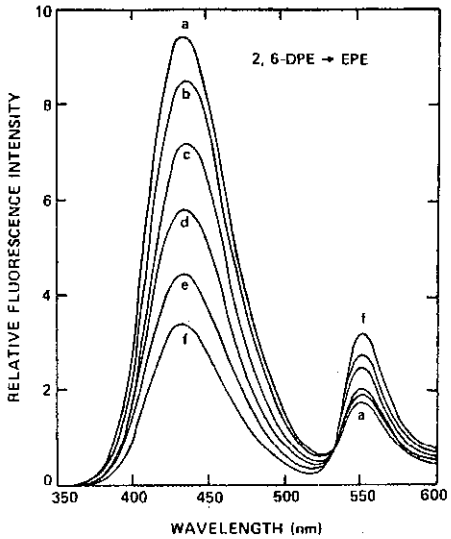

Fig 9 Emission spectra show energy transfer from 2,6-DPE to EPE in PC vesicles as a function of the ratio EPE/PC: (a) 0.001; (b) 0.002;(c) 0.005; (d) 0.10; (e) 0.013; (f) 0.016. The ratio of 2,6-DPE to EPE was kept constant at 5:1. The decrease in emission intensity at 435 nm (2,6-DPE) is accompanied by an increase at 550 nm (EPE).

The final constraint on energy transfer forms the basis of a technique for determining the lipid distribution within the membrane.

In a planar micelle, the distance between donor and acceptor at an energy transfer efficiency of 50% is calculated from the equation

$$R_o = (JK^2Qn^{-4})^{1/6} \times 9.79 \times 10^3 \qquad (1)$$

Here J is the spectral overlap integral of donor and acceptor, K^2 the dipole orientation factor, Q the quantum yield of the acceptor in the absence of the donor, and n is the refractive index of the medium.

The efficiency of energy transfer, on the other hand, can be calculated from

$$E = 1 - (1/\tau_o) \int_0^\infty e^{-t/\tau_o}\, e^{-\sigma S(t)}\, dt \qquad (2)$$

where

$$S(t) = \int_\rho^\infty \{1 - e^{-(t/\tau_o)(R_o/r)^6}\}\, 2\pi r dr \qquad (3)$$

Expressed as a function of time scaled by the lifetime of the donor's unperturbed state (t/τ_o) equation 2 and 3 show that the efficiency of energy transfer depends only on the three variables R_o, σ (the surface density of the acceptor in the micelle), and ρ, the closest distance the donor and acceptor can approach each other. (In practice, it is found that the value of ρ is not critical in these calculations provided it is much smaller than R_o.) This is just the behavior observed in Fig 9.

Fig 10 traces the efficiency of energy transfer from 2,6-DPE to EPE as a function of acceptor surface density. The solid line is the best fit of the data to equation 2 above. In this case, the calculated value of R_o was 4.87 nm, while a value of 4.6 nm was actually observed.

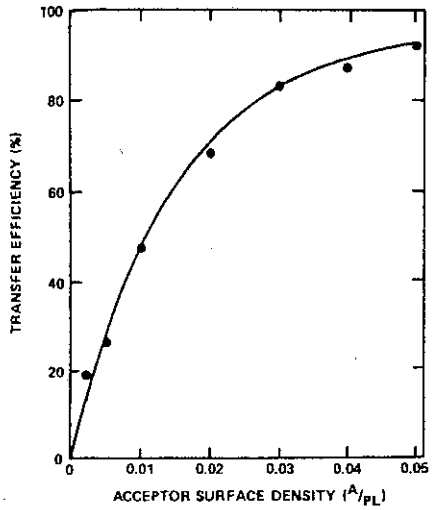

Fig 10 Energy transfer efficiency as a function of surface density of energy acceptor in PC vesicles. The solid line is a best fit of these data points to theory.

Fung and Stryer have determined the value of R_0 for a variety of lipids and so it becomes equally practical to reverse the perspective: once R_0 is known, the surface density of lipids incorporated into membranes can be found.

This series of experiments demonstrates what quantitative information can be obtained with energy-transfer spectroscopy and points the way toward mapping the distribution of lipids and proteins that is so necessary for an understanding of lipid-protein mixing during such processes as cell fusion or the clustering of lipids by antibodies.

Polarization and Conformation

Often we wish to study a subtle reaction that has no observable change in the intensity of fluorescence, or we might be concentrating on molecules with spectra so similar they cannot be resolved in time or wavelength. Polarization effects to our rescue!

When a sample is exposed to polarized light, only those molecules that are oriented preferentially will absorb energy and be excited. Similarly, the polarization vector of light emitted from a sample molecule will be oriented with that of the molecule. When a molecule remains stationary, the polarization of its emitted radiation will usually be the same as that of the exciting light. However, should the molecule rotate before it emits, the polarization will be altered accordingly. In viscous media, the amount of rotation, and corresponding change in polarization, depend directly on the size and shape of the molecule.

Applying this knowledge at the University of Illinois, Van DerLijn, Barrio and Leonard [15] investigated the enzymes of Escherichia coli, a bacterium normally resident in human intestinal tracts. And although we know more about E. coli, its various strains and mutants, than about any other cell, because of its popularity among molecular geneticists, a complete molecular model remains an elusive goal.

One of the E. coli enzymes, ATCase (aspartate transcarbamylase) is a catalyst in a reaction that initiates the pyrimidine biosynthetic pathway that eventually leads to the formation of the nucleic acids DNA and RNA. The process is activated when the nucleotide ATP (adenosine 5'-triphosphate) reacts with the ATCase. Alternately, the process is halted by the binding of CTP (cytidine 5'-triphosphate). The interesting feature of this allosteric (self-regulating) reaction is that the moderating enzymes are produced by the process: the reaction turns itself off.

Taking advantage of an analog of ATP, linear-benzo-ATP, which has an unquenched fluorescence spectrum when the molecule binds to ATCase, Van DerLijn et al determined the specific nature and types of nucleotide binding sites on ATCase.

The fidelity of this analog to the normal ATP molecule can be appreciated from Fig 11 where the activation of ATCase is plotted as a function of both the ATP and the analog concentration. The two activators prove to be equally effective throughout the concentration range.

Since there is no change in the fluorescence quantum yield when the analog binds to ATCase, binding parameters cannot be linked directly to emission intensity. However, by exciting a mixed sample of enzymes with polarized light, then viewing the emission through analyzers that alternately pass only light polarized parallel ($I_{||}$) and perpendicular ($I_{\perp}$) to the exciting radiation, we can define the degree of polarization (P) and the fraction of linear-benzo-ATP (lbATP) bound to ATCase (X) as

$$P = (I_{||} - I_{\perp})/(I_{||} + I_{\perp})$$

$$X = 1 - I(P_B - P)/I_o(P_B - P_F)$$

where P, P_F, P_B are the polarization of lbATP in the presence, absence and bound to ATCase, while I_o and I are the fluorescence intensities of lbATP solutions before and after the addition of ATCase.

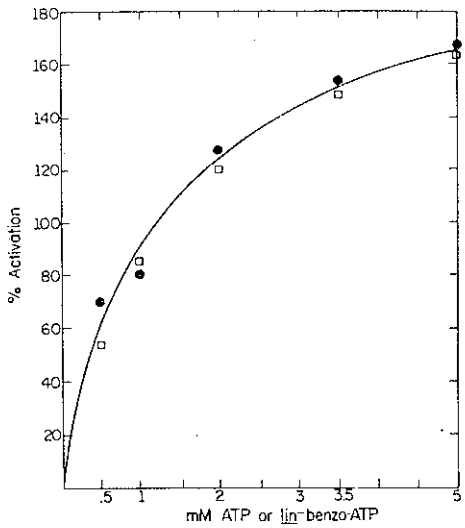

Fig 11 Activation of the enzyme ATCase as a function of ATP and linear-benzo-ATP concentration showing the fidelity of the analog to the actual nucleotide.

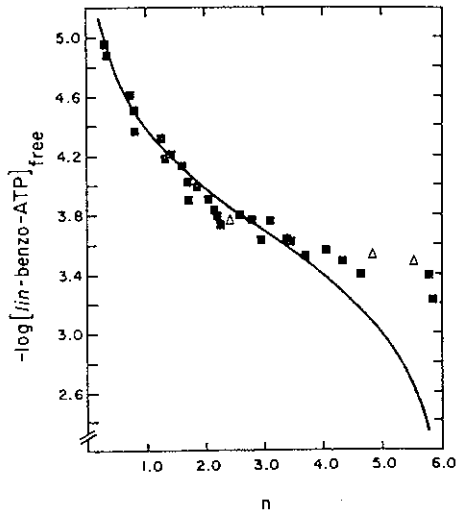

Fig 12 Bjerrum plot of lbATP binding to ATCase from data taken with the FLUOROLOG's polarization kit. The solid line is a computer-generated curve and the triangular points were taken in a slightly altered environment.

The number of molecules of lbATP bound per ATCase is

$$n = X(lbATP)_{total}/(ATCase)_{total}$$

while the free concentration is

$$(lbATP)_{free} = (1 - X)(lbATP)_{total}$$

Data from polarization studies performed with the FLUOROLOG's polarization kit is plotted in Fig 12 according to the Bjerrum equation

$$\log (n/N-n) = \log K_a + \log (lbATP)_{free}$$

where N is the number of binding sites (six for ATCase) and K_a is the association constant that is a direct measure of the binding strength of the system. Obviously, when $n = 3$, k_a is equal to the reciprocal of the free lbATP concentration. The solid line in the figure is a computer-fitted binding curve that yields $K_a = 5 \times 10^3\ M^{-1}$.

The average angle of rotation (ω) of the analog-enzyme system can be calculated from

$$\frac{1}{P_B} - \frac{1}{3} = \left\{\frac{1}{P_o} - \frac{1}{3}\right\} \frac{2}{3\cos^2\omega - 1}$$

where P_o is the intrinsic polarization of the fluorophor. From the experimental data, the average angle of rotation of the probe-bound ATCase was found to be about 35 degrees. Theoretically, however, a molecule of this size should rotate only 9.5 degrees during the lifetime of the analog excited state. This apparent discrepancy can be resolved only if nucleotides bind loosely at the allosteric sites of ATCase and the bonds are flexible enough to allow expansion, lateral extension, and freedom to rotate. This rotational character suggests the lbATP molecule has a single point of attachment at the ATCase allosteric site.

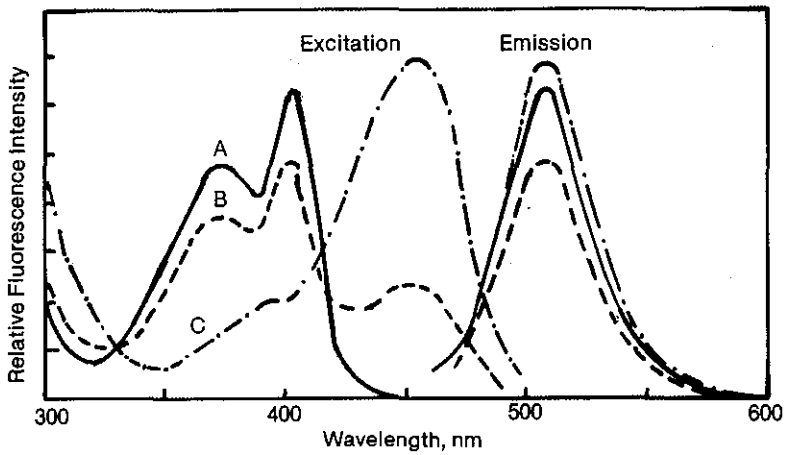

Fig 13 Excitation and emission spectra of pyranine at pH 4 (A), 7 (B), 10 (C) indicating extreme dependence on hydrogen ion concentration. Samples were maintained at a constant temperature with the FLUOROLOG's variable temperature accessory.

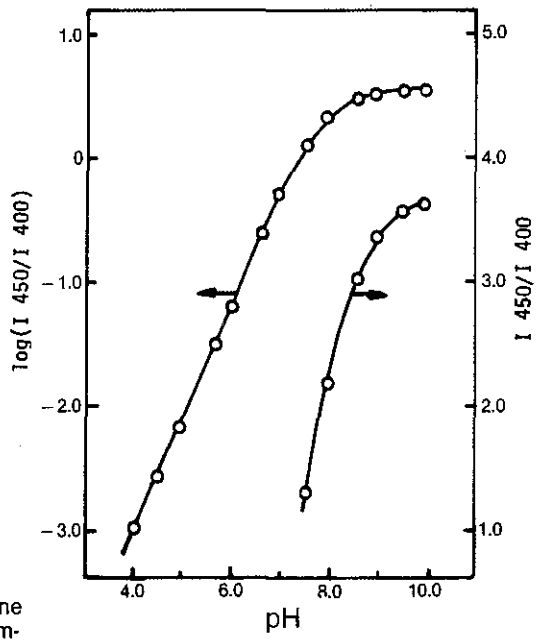

Fig 14 Ratios of relative intensities of the 450 and 400 nm peaks in the excitation spectra of pyranine as a function of pH. The calibration was performed while viewing the emission line et 510 nm.

Proton Gradients

Besides serving as an activator, ATP plays a pivotal role in all cellular metabolism. A product of both photosynthesis and respiration, it is the main distributor and carrier of energy. In aerobic cells, ADP (adenosine 5'-diphosphate) is phosphorilized into the higher energy phosphate group of ATP at the inner membrane of the mitochodrion. The chemosomatic coupling hypotheses proposes a proton gradient across the cell membrane as responsible for this synthetic reaction. To verify such a claim, it is imperative to find a way to monitor the pH in cell interiors.

Kano and Fendler [16], in the course of examining lipid-modulated drug delivery, demonstrated pyranine to be a convenient and sensitive probe of the surface and interior pH of phospholipid vesicles. Fig 13 shows the excitation and emission spectra of pyranine for various pH values. Note how strongly the peaks in the excitation spectra at 400 and 450 nm depend on the hydrogen ion concentration.

The pyranine reaction was calibrated (Fig 14) by running the excitation spectra at various pH values. Over the pH range from 4 to 10, the intensity ratio of the 450 nm peak to that at 400 nm ranged over four orders of magnitude, evidence of the extreme sensitivity of the probe.

Once entrapped by the vesicles, pyranine does not easily diffuse through the membrane and leakage was less than 1% per day. Most important, quenchers, usually existing in biological materials and playing havoc with emission-dependent probes, do not affect the intensity ratios of excitation spectra and pH values are immune to this major source of error. As a bonus, the polarization of pyranine fluorescence is a good indicator of the microviscosity of the medium it inhabits.

Table 1 includes a partial list of pH gradients for single and multicompartment vesicles in various buffers.

Further repercussions of the work can be found in observations of viruses, those molecular complexes that are virtually dead until they penetrate a living cell and appropriate the cell's metabolic machinery. It has been established that the way proteins aggregate to form viruses is strongly dependent on the pH of the surroundings [17], so an accurate measurement of proton concentration will be invaluable for achievement of weapons against viral diseases from rabies to influenza - and possibly cancer.

On the Horizon

The sophisticated luminescence measurements of the FLUOROLOG, of course, aren't the only windows into the cell. Raman, ESR, and NMR spectroscopies, along with a host of other tools, have contributed their shares to our present knowledge of cytology and biochemistry. On the other hand, the cell is but one of many vistas exposed by the FLUOROLOG. A panorama of other applications, from laser dyes to high-resolution pyrene fluorescence to monolayers as thin as 2 nm is beginning to unfold. We'll try to keep you posted.

TABLE 1

pH gradients across membranes for single (S) and multicompartment (M) vesicles in various buffers. Outer pH values determined with a combination electrode.

Vesicle	Buffer	pH (outer)	pH (inner)
S	sodium borate	9.87	8.1
S	sodium phosphate	7.63	7.4
M	sodium acetate	6.16	6.0
M	HCl	2.00	6.4

REFERENCES

1. The Spex Speaker, Vol XXI, No 3, 1 (1976)
2. The Spex Speaker, Vol XX, No 4, 1 (1976)
3. C.P. Swanson, The Cell, Prentice-Hall, Inc., Englewood Cliffs, NJ (1963)
4. In press
5. The Spex Speaker, Vol XXII, No 4 (1977)
6. J.D. Winefordner, S.G. Schulman, T.C. O'Haver, Luminescence Spectrometry in Analytical Chemistry, Wiley-Interscience, NY (1972)
7. N.J. Turro, K. Liu, M. Chow, P. Lee, PhotoChem. Photobio. **27**, 525 (1978)
8. J.R. Escabi-Perez, N. Faruk, J.H. Fendler, J. Am. Chem. Soc. **99**, 7749 (1977)
9. S.A. Alkaitis, M. Gratzel, Ber. Bunsenges. Phys. Chem. **79**, 541 (1975)
10. S.A. Alkaitis, M. Gratzel, J. Am. Chem. Soc. **98**, 3549 (1976)
11. A.J. Pesce, C. Rosen, T.L. Pasby, Fluoresence Spectroscopy, Marcel Dekker, Inc., NY (1971)
12. B.K. Fung, L. Stryer, Biochem. **17**, 24, 5241 (1978)
13. C. Tanford, The Hydrophobic Effect, John Wiley & Sons, NY (1973)
14. L. Stryer, Radiation Res. Suppl. **2**, 432 (1960)
15. P. Van DerLijn, J.R. Barrio, N.J. Leonard, J. Biol. Chem. **253**, 24, 8694 (1978)
16. K. Kano, J.H. Fendler, Biochem. et Biophys. Acta **509**, 289 (1978)
17. P.J.G. Butler, A. Klug, Scientific American 239, 5 (1978)

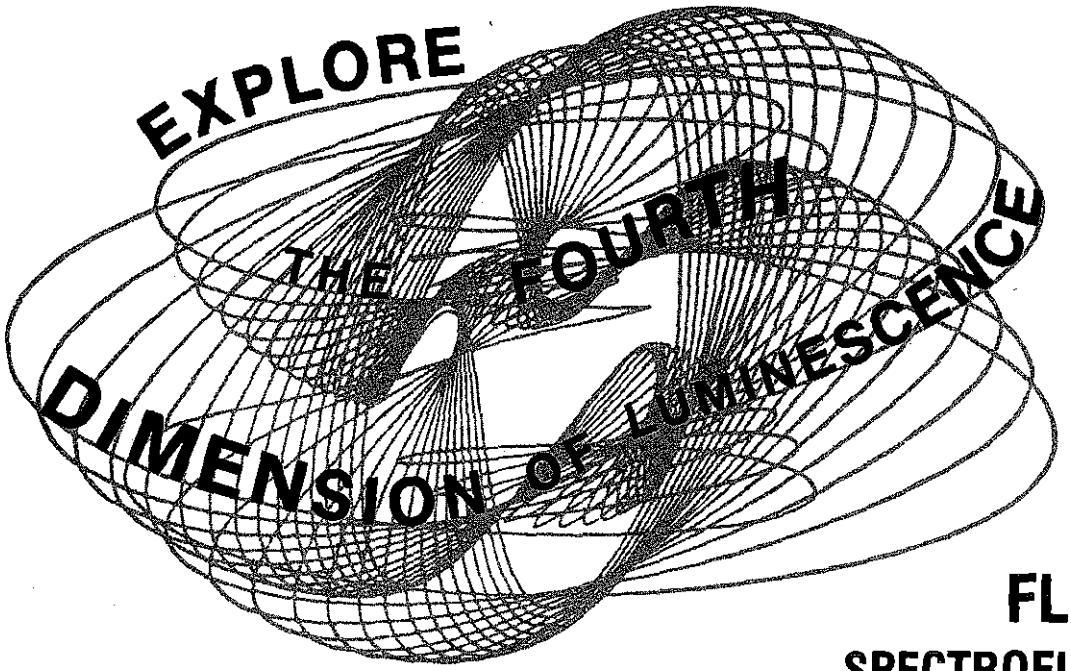

WITH THE

SPEX

FLUOROLOG

SPECTROFLUOROMETER

AND UNIQUE PULSED-LAMP PHOSPHORIMETER

FOR

ADDED DIMENSION:

SCAMP

THE AFFORDABLE

System
Controller and data
Acquisition
Monitor
Processor

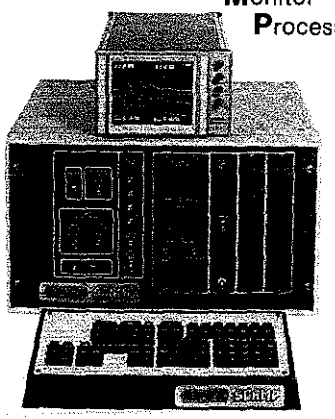

At less than half the cost of computerized systems, the SCAMP converts your lab into a powerful instruments system. Accepting BCD or analog data from **any** instrument, spectrometer to chromatograph, the SCAMP provides *all* the routines you need to display and refine raw data into real information **WITHOUT THE FRUSTRATIONS OF PROGRAMMING AND INTERFACING.**

Isolate time-dependent emissions with as little as 1 μsec between excitation and emission. A pulsed xenon flash-lamp combined with high-precision processing circuitry has created an extremely versatile and accomodating instrument. Delays are variable from 1 μsec to 10msec; sampling times from 10 μsec to 0.9 sec, with data accumulated up to 99 flashes.

UNSURPASSED FOR HANDLING EASE AND ACCURACY IN:

- .. LIFETIME DETERMINATIONS
- .. TIME RESOLUTIONS OF A MIXTURE OF COMPONENTS
- .. IMPLEMENTING PHOSPHORESCENT IONS AS ENVIRONMENTAL PROBES

1902 FLUOROLOG

1934 PHOSPHORIMETER

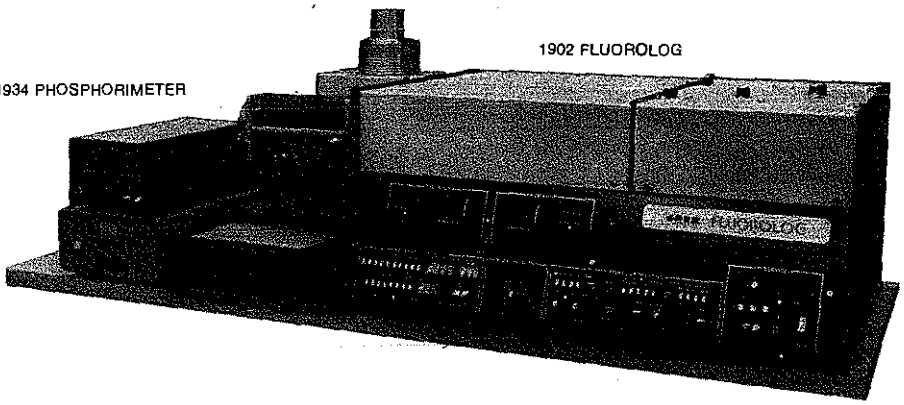

ONLY SPEX FLUOROLOG HAS:

- .. TWO DOUBLE MONOCHROMATORS
- .. PHOTON COUNTING DETECTION
- .. BOX-CAR INTEGRATION BY DIGITAL ELECTRONICS
- .. LARGE, REMOVABLE SAMPLE COMPARTMENT
- .. MODULAR CONSTRUCTION FOR FLEXIBILITY WITH SOURCES AND DETECTORS

Put them to the test
Call us for a Demo

SPEX INDUSTRIES, INC./ P.O. BOX 798/METUCHEN, N. J. 08840/ ☎ (201) 549-7144

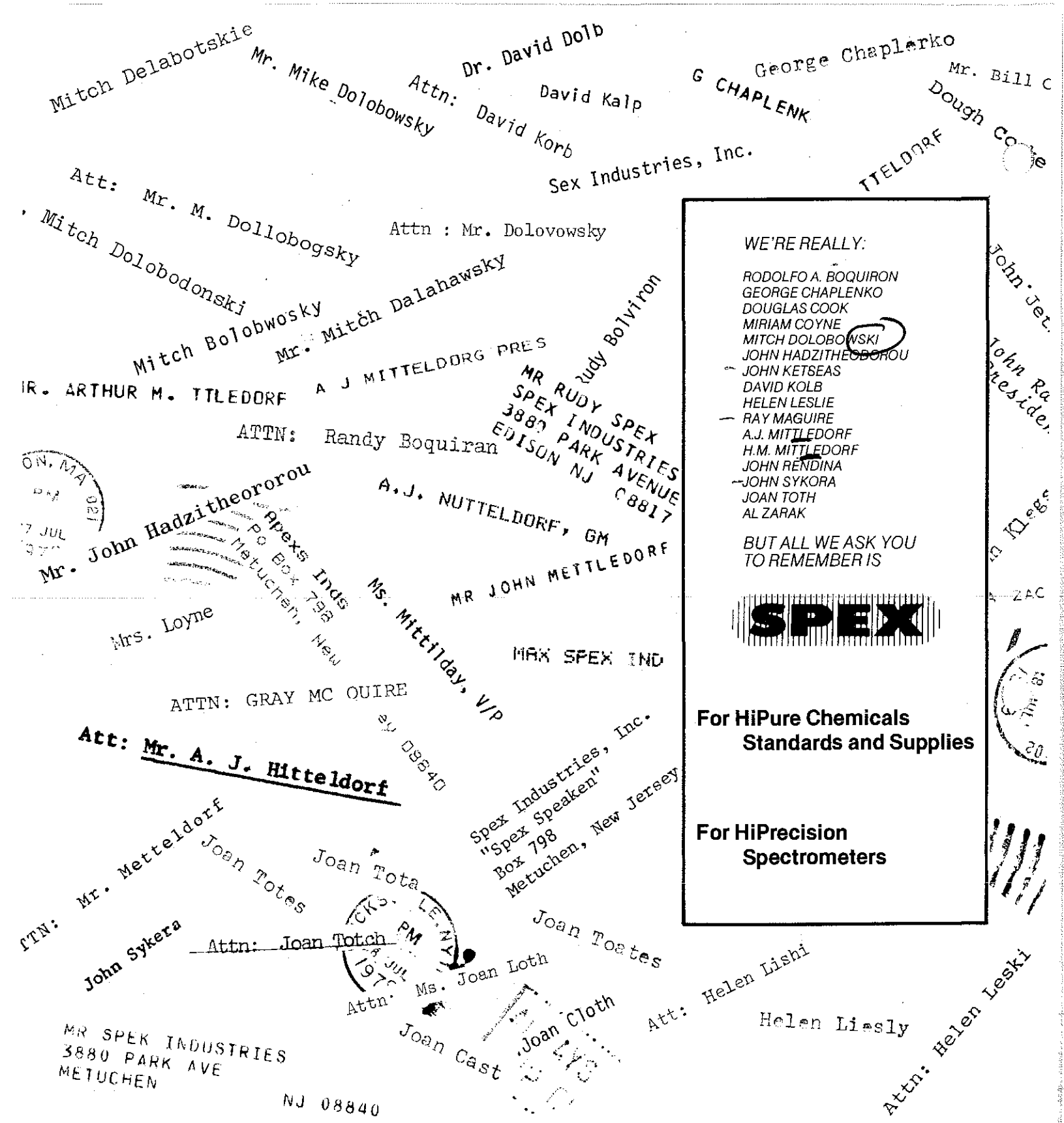

WE'RE REALLY:

RODOLFO A. BOQUIRON
GEORGE CHAPLENKO
DOUGLAS COOK
MIRIAM COYNE
MITCH DOLOBOWSKI
JOHN HADZITHEODOROU
JOHN KETSEAS
DAVID KOLB
HELEN LESLIE
RAY MAGUIRE
A.J. MITTLEDORF
H.M. MITTLEDORF
JOHN RENDINA
JOHN SYKORA
JOAN TOTH
AL ZARAK

BUT ALL WE ASK YOU TO REMEMBER IS

SPEX

For HiPure Chemicals Standards and Supplies

For HiPrecision Spectrometers

SPEX INDUSTRIES, INC. • BOX 798, METUCHEN, N.J. 08840 • ☎(201)-549-7144

WESTERN REGIONAL OFFICE: 3246 McKINLEY DR., SANTA CLARA, CA. 95051 408/246-2333

AMBRIEX S.A.
Rua Tupi 535, 01233
Sao Paulo
BRAZIL

GLEN CRESTON
16 Carlisle Road
London, NW9 OHL
ENGLAND

INSTRUMENTALIA S.R.L.
P.O.B. 7
1114 Buenos Aires
ARGENTINA

QUENTRON OPTICS PTY. LTD.
576-578 Port Road
Allenby Gardens
SOUTH AUSTRALIA 5009

SEISHIN TRADING CO.
43, Sannomiya-cho
1-chome, Ikuta-ku
Kobe, JAPAN

EQUILAB C.A.
Apartado 60.497
Caracas 106
VENEZUELA

HARVIN AGENCIES
C-7 & 8, Industrial Estate
Sanantnagar
Hyderabad -500018 AP INDIA

LANDSEAS (ISRAEL) LTD.
38, King George Street
Tel Aviv
ISRAEL

RADIONICS LTD.
195 Rue Graveline
Montreal
H4T 1R6 CANADA

SPEX INDUSTRIES, GMBH
Iblherstrasse 53
D8000 Munchen 83
WEST GERMANY